Academic Journal of Science and Technology
ISSN: 2771-3032 | Vol. 9, No. 3, 2024

Study on the Speed Control and Heat Dissipation Performance of Cone-tube Permanent Magnet Governor

Yonglang Hong[1, *], Weiren Zhao[2], Xing Chen[3], Senjie Ruan[4]

[1] Electronic Science and Technology, Guangdong University of Technology, Guangdong 510006, China
[2] Electronic Science and Technology, Guangdong University of Technology, Guangdong 510006, China
[3] Intermediate Engineer, Zhuji Hechuang Electric Technology Co., LTD. Zhejiang 311800, China
[4] Intermediate Engineer, Zhuji Hechuang Electric Technology Co., LTD. Zhejiang 311800, China
[*] Corresponding author: Weiren Zhao (Email: zwrab@163.com)

Abstract: The speed regulation range, output torque, and heat dissipation performance are important performance indicators of permanent magnet speed regulators. Enhancing the speed regulation range and output torque, and reducing the heat generation power are of significant importance for expanding the application range of permanent magnet speed regulators. To address the issues of a single adjustment process, insufficient heat dissipation space, and inadequate torque transmission capability of the traditional straight-barrel permanent magnet speed regulator, a cone-barrel permanent magnet speed regulator with a magnetic rotor assembly structure was designed through the analysis of the structure and transmission characteristics of the traditional straight-barrel permanent magnet speed regulator. Using the ANSYS Maxwell finite element analysis software, the output torque characteristics of the cone-barrel structure were studied. Considering the effect of eddy current heating, a conjugate heat transfer model for the permanent magnet speed regulator was developed, and the heat dissipation performance of the cone-barrel structure was explored through ANSYS Fluent simulation analysis. The results indicate that compared to the traditional straight-barrel permanent magnet speed regulator, the cone-barrel regulator can provide greater output torque when fully coupled; at maximum power consumption, the air velocity over the surface of the cone-barrel permanent magnet speed regulator conductor is higher, resulting in better heat dissipation and thus a lower operating temperature.

Keywords: Permanent magnet speed regulator, fan load, speed regulation performance, heat dissipation.

1. Introduction

Due to the adoption of a purely mechanical mechanism, permanent magnet speed regulators are free from the power harmonics and electromagnetic interference associated with speed control mechanisms like frequency converters. With their unique soft start and overload protection, they have been widely applied in industrial fields such as military, chemical, mining, and power generation, where load power is high, working environments are complex, and safety and reliability requirements are stringent, including applications in fans, pumps, and industrial equipment[1].

To improve the performance of permanent magnet speed regulators, extensive research has been conducted. Wang[2] used a bidirectional coupling calculation method to study the temperature distribution of speed regulators during operation, and experimental evidence showed that the results of bidirectional coupling calculations are closer to the actual values. Qi[3] and others analyzed the electromagnetic and temperature fields of disc-type permanent magnet speed regulators, studied the impact of various parameters on electromagnetic torque, and proposed increasing heat dissipation for disc-type regulators experiencing high temperatures. They simulated the temperature distribution of the regulator's conductor and permanent magnets after adding heat dissipation fins, and the results showed that the temperature of both the permanent magnets and the conductor decreased, meeting the temperature safety standards. Wang[4] and other scholars conducted a heat dissipation analysis on cylinder-type speed regulators, utilizing finite element analysis and orthogonal experimental methods to study the effects of structural parameters such as the fin length and angle of heat dissipation fins on the cooling effect, and identified the optimal fin height, spacing, and axial angle to be 21mm, 9mm, and 37°, respectively. Li[5] designed a speed regulator with an adjustable magnetic ring structure, which can achieve speed regulation within a certain range without changing the coupling degree or air gap, simply by moving the magnetic ring. Wu[6] proposed a segmented conductor permanent magnet speed regulator, which, while sacrificing some torque, achieves a more uniform speed regulation range with the change of coupling degree and a more unique working point under different coupling degrees.

Although these studies have enhanced the understanding of the speed regulation patterns and heat dissipation characteristics of speed regulators, how to further increase the speed regulation range and improve heat dissipation performance remains the biggest challenge facing permanent magnet speed regulators. For example, in the speed regulation process of fan and pump machines, as the slip increases, the torque of the permanent magnet speed regulator continuously decreases, and the slip power[7] first increases and then decreases, making it difficult to meet the application requirements of high-power speed regulators. Existing speed regulators only adjust the eddy current size to achieve speed regulation by adjusting the coupling degree or changing the air gap. On the basis of conventional cylindrical permanent magnet regulator structures, a permanent magnet speed regulator structure composed of a cone-barrel conductor and irregular trapezoidal permanent magnets was designed. This structure allows for the simultaneous change of coupling degree and air gap. Finite element simulation software[8] was used to simulate and calculate the electromagnetic characteristics and temperature characteristics of this speed

regulator structure. The output speed, output power, flow field distribution on the surface of the conductor rotor, heat transfer coefficient, and temperature distribution of the conductor rotor were calculated and compared with those of the conventional straight-barrel permanent magnet speed regulator.

2. Structural Design

The commonly used permanent magnet speed regulator is a straight-barrel type, consisting of a magnetic rotor, a conductor rotor, and regulating devices, as shown in Figure 1(a). The conductor rotor is connected to the motor shaft, and the magnetic rotor is connected to the load shaft. Permanent magnets are mounted on the outer surface of the inner rotor yoke cylinder, magnetized radially, with adjacent permanent magnets magnetized in opposite directions. During operation, the motor drives the conductor rotor to rotate, causing relative displacement with the magnetic rotor. Eddy currents and an induced magnetic field form on the surface of the conductor, interacting and driving the magnetic rotor to rotate. When the magnetic rotor moves outward along the axial direction, the eddy current area decreases, the induced magnetic field weakens, and the speed of the magnetic rotor decreases, achieving the purpose of speed regulation[9].

This article proposes a speed regulator combining a conical barrel conductor with trapezoidal permanent magnets, as shown in Figure 1(b). Compared with the conventional cylindrical permanent magnet speed regulator shown in Figure 1(a), this design reduces the thickness(d_4) of one end of the traditional rectangular permanent magnet but increases its width(d_2), making the cross-section of the permanent magnet trapezoidal while keeping the overall volume unchanged for comparison with the traditional rectangular permanent magnet scenario. The shape of the trapezoidal permanent magnet is shown on the right side of Figure 1(b).

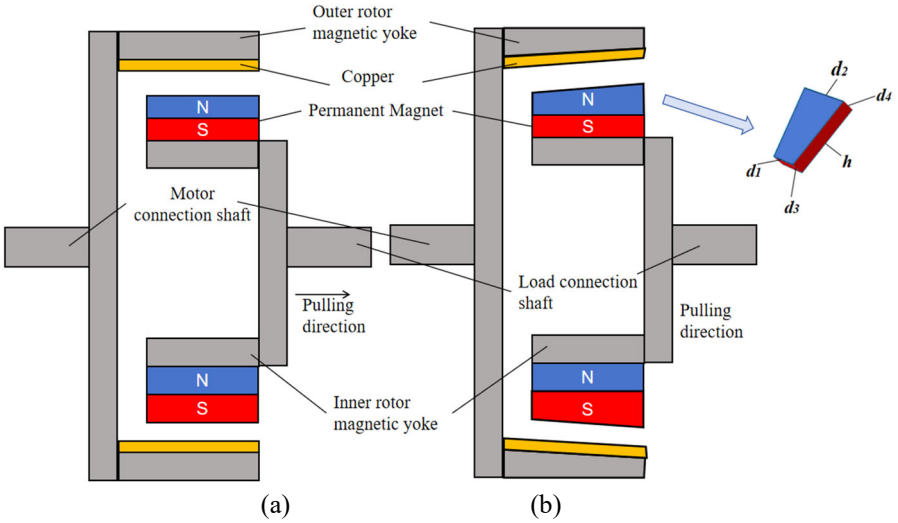

Figure 1. Section drawing of straight cylinder permanent magnet governor(a) and Permanent magnet governor-cone structure profile and permanent magnet drawing(b)

3. Electromagnetic performance simulation

3.1. Condition setting

Construct a simplified model using finite element electromagnetic simulation software. The yoke iron material is set to steel_1010 from the material library, and the conductor material is set to copper; the motor speed is set to 1480 rpm. The structural parameters of the straight-barrel type speed regulator are shown in Table 1, and the related performance parameters are shown in Table 2. Based on the model dimensions and material properties, and ensuring a uniform air gap width of 7mm between the magnetic rotor and the conductor rotor when fully coupled, establish a simulation model of the conical barrel permanent magnet speed regulator. Under the condition that the volume, base size, and height of the permanent magnet remain unchanged, change the length and width of the top of the permanent magnet to conduct simulation research on the speed regulator.

Table 1. parameters of the permanent magnet governor

Symbol	Definition	Value
r_0	Outer diameter of the permanent magnet yoke rotor	530rpm
l_r	Permanent magnet thickness	30mm
l_1	Permanent magnet width	40mm
l_2	Permanent magnet length	100mm
p	Permanent magnet pole logarithm	10
l_c	Thickness of conductor cylinder	6mm
l_3	Length of conductor cylinder	145mm
l_a	width of air gap	7mm
l_s	Magnet yoke iron thickness	25mm

Table 2. Material property Parameters

Symbol	Definition	Value
μ_0	Permeability of vacuum	$4\pi\times10^{-7}N\cdot A^{-2}$
B_r	Permanent Magnet Remanence	1.22T
H_r	Coercivity of permanent magnet	876kA/m
μ_r	Relative permeability of permanent magnet	1.10827
σ	Electrical conductivity of copper	4.96×10^7S/m
μ_{rc}	Relative permeability of copper	0.999991

The changes in the permanent magnet size structural parameters are shown in Table 3, where the first type is the conventional straight-barrel, and the latter three conical barrel types are marked as Models A, B, and C, respectively.

Table 3. Permanent magnet size and volume parameters

Symbol	Definition	Unit	Straight tube type	A model	B model	C model
d_1	Bottom length	mm	40	40	40	40
d_2	Bottom width	mm	30	30	30	30
h	Height	mm	100	100	100	100
d_3	Top length	mm	40	45	50	55
d_4	Top width	mm	30	26.54	23.57	21
V	Volume	mm^3	1.2×10^5	1.2×10^5	1.2×10^5	1.2×10^5

The relationship between the output power P of the speed regulator and the magnetic rotor speed n, and the torque T experienced by the magnetic rotor is as follows:

$$P=\frac{n\pi T}{30} \tag{3-1}$$

The load torque of the fan and pump is directly proportional to the square of the speed[10], and a centrifugal load with a rated power of 90kW is chosen for the experiment. The relationship between the resistance torque T' experienced by the magnetic rotor and its speed n is as follows:

$$T'=kn^2 \tag{3-2}$$

With an active shaft speed of 1480rpm, and the load at 4% rated slip, the rated torque is approximately 604.9N·m. By combining (3-1) and (3-2), the load coefficient k is calculated to be 2.99673×10^{-4}.

3.2. Simulation results and discussion

The dashed lines in Figure 2 represent the relationship between the load speed n and the torque T' under different coupling degrees for Model A speed regulator. ***a'***, ***b'***, ***c'***, ***d'***, and ***e'*** are the intersection points of the speed regulator's operating points with the load curve, where the conductor rotor and the magnetic rotor are coupled at 100%, 80%, 60%, 40%, and 20% respectively. For comparison, the speed and torque curves of the straight-barrel speed regulator and its intersection points with the load curve, ***a***, ***b***, ***c***, ***d***, and ***e***, are also shown. Intersection points ***a*** and ***a'*** are both the operating points of the speed regulator at 100% coupling degree. For the straight-barrel speed regulator, the output speed at point a reaches 1421.34 rpm, and the output torque reaches 604.98N·m. By formula (3-1), the output power at point a is approximately 90.04kW. However, for the conical barrel speed regulator, the output speed at point a reaches 1424.76 rpm, and the output torque reaches 608.31N·m, both of which are higher than those of the conventional straight-barrel speed regulator.

As the coupling degree decreases, the operating point gradually moves from ***a*** to ***e***. Since there is only one operating point for each coupling degree, the straight-barrel speed regulator can achieve a relatively stable speed adjustment from 0 to 1421.34 rpm, while the conical barrel structure A can achieve a relatively stable speed adjustment from 0 to 1424.76 rpm. Therefore, the speed adjustment range of the conical barrel speed regulator is slightly larger than that of the straight-barrel speed regulator.

As shown in Figure 2, at approximately 60% to 100% coupling degree, the output torque of the conical structure is greater than that of the straight structure, whereas at approximately 0% to 60% coupling degree, the output torque of the straight structure is greater than that of the conical structure. This indicates that the conical structure has advantages over the straight structure when high torque output is required.

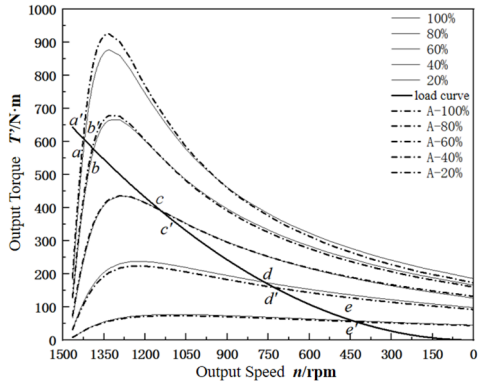

Figure 2. Output torque characteristic curve of different coupling degree between model A and straight cylinder governor

Figure 3 shows the relationship between the output speed and coupling degree of the straight-barrel and three types of conical barrel speed regulators. The trend curves formed by connecting ten calculation points for each structure show that at high coupling degrees, the output speed of the conical structure is higher, and at low coupling degrees, the output speed of the conical structure is lower. Since the output speed of the permanent magnet speed regulator decreases with the reduction of the

coupling degree, points ***a***, ***b***, and ***c*** in Figure 3 are the intersection points of the trend lines for conical structures A, B, and C with the straight-barrel speed regulator trend line. The larger the cone angle, the faster the speed decreases. From the positions of points ***a***, ***b***, and ***c***, it can be seen that the larger the cone angle, the higher the coupling degree at the intersection point. Therefore, between 20% and 100% coupling degrees, the larger the cone angle of the conical barrel speed regulator, the greater the speed adjustment range. Hence, the larger the cone angle of the conical barrel speed regulator, the wider the speed adjustment range.

Figure 4 shows the relationship between the output power and coupling degree of the straight-barrel and three types of conical barrel speed regulators. The trend curve obtained by connecting ten calculation points indicates that both for the straight-barrel and the conical barrel, the trend of output power variation with coupling degree is similar to the change in output speed. At low coupling degrees, the output power of the conical structure is higher; at high coupling degrees, the output power of the conical structure is lower. The larger the cone angle of the conical structure, the wider the power range.

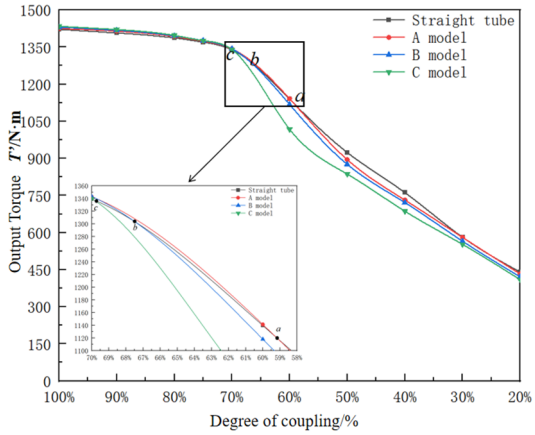

Figure 3. The output speed of different structures varies with the coupling degree

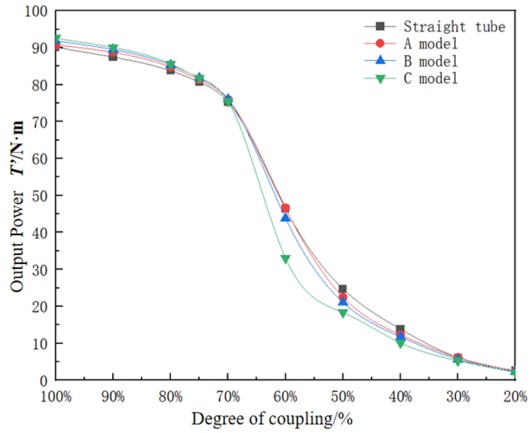

Figure 4. Power power of different structures with coupling degree

4. Radiation Analysis

To import the eddy current loss from the magnetic field simulation result file into the initial settings for the temperature field analysis, magnetic-thermal coupling simulation is performed using the ANSYS Maxwell 3D module and Fluent module, with the relationship diagram established in Workbench as shown in Figure 5.

Figure 5 Unidirectional magnetic-thermal coupling

The temperature rise caused by the eddy current loss generated through magnetic-thermal coupling analysis is studied and compared in terms of heating and cooling conditions between the conical and straight-barrel structures.

Based on the structure of the speed regulator, the variation curve of the air gap width between the magnetic rotor and the conductor rotor under different structures can be obtained as it changes with their coupling degree, as shown in Figure 6.

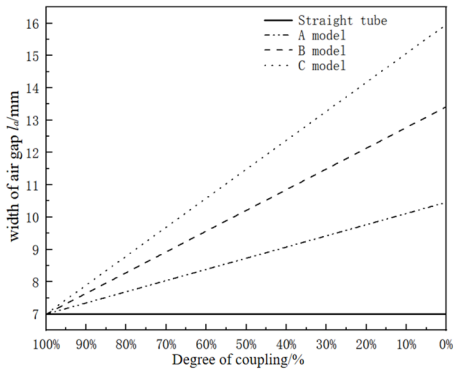

Figure 6. Curve of air gap width change with coupling degree under different structures

The air gap width of the straight-barrel structure remains unchanged at 7mm, while the air gap width of the conical structure continuously increases as the coupling degree decreases. When fully coupled, the air gap width of all structures is equal, but when completely disengaged, the air gap widths of models A, B, and C increase by 49.42%, 91.65%, and 128.05%, respectively, compared to the straight-barrel structure. The larger the gap, the greater the cooling space.

In permanent magnet speed regulators, there are mainly two modes of heat transfer:conduction and convection [11]. According to the law of energy conservation, the heat transferred by the solid wall is equal to the heat absorbed by the fluid [12-14], and the energy equation for the fluid-solid coupling is as follows:

$$\lambda\left(\frac{\partial T}{\partial n}\right)=h\left(T_w-T_f\right) \tag{3-1}$$

In the equation, λ represents the thermal conductivity of the solid, $\partial T/\partial n$ represents the change in temperature per unit thickness, T_w represents the wall temperature; T_f represents the fluid temperature; h represents the convective heat

transfer coefficient at the fluid-solid interface.

The heat transfer mode of the wall is set to coupled heat transfer. The external structure of the heat dissipation and grid division is established as shown in Figure 7. The ambient temperature of the air is set to 26.85°C.

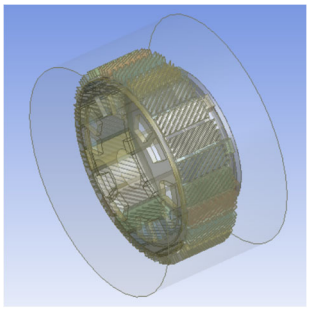

Figure 7. Heat dissipation structure model

Only the rotor part is changed to adopt straight-barrel or conical barrel Models A, B, C. Analyze the temperature distribution under different models and coupling degrees, with the material property parameters set as follows:

Table 4. Material attribute parameters

Structure	Material	Density (kg/m^3)	Specific heat capacity (Jkg /°C)	thermal conductivity (W/(m °C))
Yoke iron	Iron	7870	460	80
Fluid	Air	1.18	1042	0.0317
Conductor tube	Copper	8900	386	401
permanent magnet	Rubidium iron boron	8400	504	8
Flange plate	Aluminium	2720	880	237
heat sink	Aluminium	2720	880	237

4.1. Thermal power analysis

Since the thermal power consumption of the centrifugal load is only related to the slip and reaches its maximum value—4/27 times the rated power—at 1/3 slip, for an active end speed of 1480rpm, the maximum thermal power consumption at a load of 90kW occurs at 986.67rpm, approximately 13.5kW [15].

Figure 8 shows the eddy current thermal power consumption distribution in the conductor rotor and permanent magnet rotor at maximum power consumption obtained through finite element analysis. Figures 8(a), (b), (c), and (d) correspond to the eddy current thermal power consumption distribution at maximum thermal power consumption of the straight-barrel, conical barrel Models A, B, and C, respectively. At this thermal loss, the coupling area to reach maximum thermal power consumption becomes larger, and the maximum unit volume heating power decreases to 4.57×10^{8}W/m3. It can be seen that due to the increase in air gap with decreasing coupling degree, the conical structure causes the output power to decrease faster than the straight structure, making the coupling degree at which maximum thermal power consumption is reached greater, with the coupling degree affecting the eddy current area. The larger the eddy current area, the smaller the unit volume thermal loss.

degrees of the straight-barrel, conical barrel Models A, B, and C are respectively 52.49%, 53.31%, 55.22%, 58.97%. During operation, the instantaneous unit volume heating power generated by eddy currents at the position directly opposite the conductor rotor and the magnet pole is the highest. Overall, the eddy current distribution situation of the conical and straight-barrel structures is similar, with most of the thermal loss located in the conductor rotor, and the heating power of the permanent magnet is lower. From the volume distribution of eddy current loss, it can be seen that at the same slip power, the conical structure requires a greater coupling degree to reach maximum thermal power consumption, resulting in a smaller maximum unit volume heating power, with the straight structure reaching up to 7.49×10^{8}W/m3, while conical structure A reaches up to 5.83×10^{8}W/m3. As the cone angle increases, the coupling surface

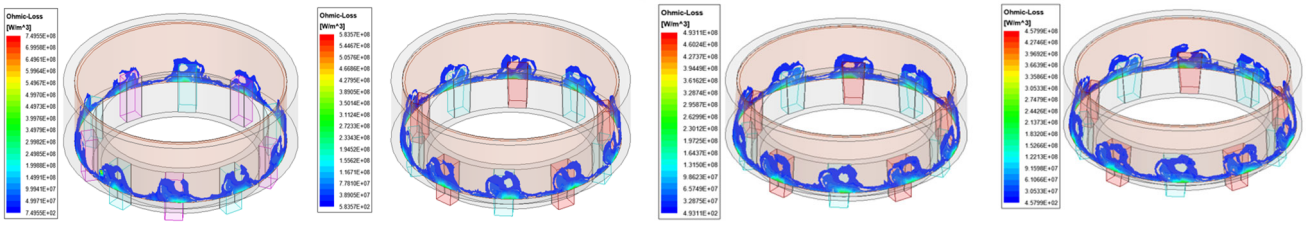

(a)Straight tube structure (b)A model (c)B model (d)C model

Figure 8 Distribution of eddy current loss of different structures of permanent magnet governor under maximum power consumption

4.2. Flow field analysis results

Figure 9 shows the distribution of surface velocity vectors on the conductor at a rotor speed of 1480rpm under different structures. Figure 9(a) displays the velocity distribution on the surface of a straight-barrel structure, revealing values between 36.26 to 36.37m/s, consistent with the linear speed of the internal surface particles of the conductor at the corresponding speed. Near the end faces, due to air viscosity, the linear speed is greater, approaching 37.23m/s. Figures 9(b), (c), and (d) illustrate the surface velocity vector distribution for conical barrel structures A, B, and C, respectively. It is observed that the special structure of the conical barrel results in higher linear speeds near the magnet brick end, creating a larger velocity gradient. As the taper increases, the speed near the end face of the permanent magnet rotor increases, with the maximum surface speed ranging from 37.99m/s to 39.16m/s. This increases the air flow speed near the surface of the conductor at the permanent magnet end. Since convective heat transfer effectiveness is related to the gas flow speed at the interface, employing a conical barrel structure enhances the heat transfer effect.

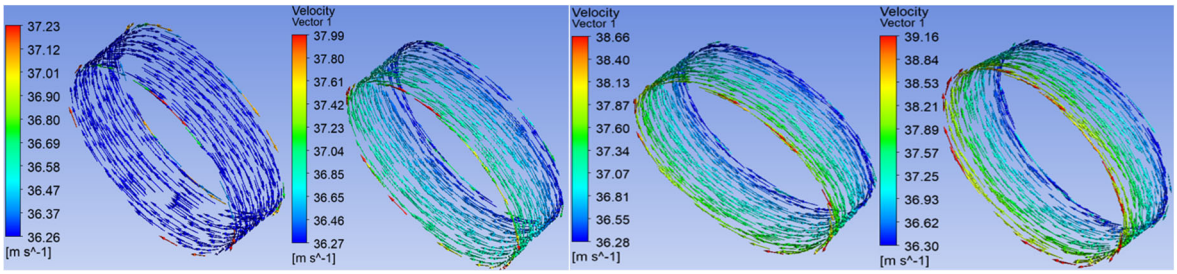

(a)Straight tube structure (b)A model (c)B model (d)C model

Figure 9. Distribution of the conductor surface velocity vector under different structures

4.3. Temperature Field Analysis Results

Figure 10 presents the temperature distribution of the conductor rotor under maximum thermal power loss for different structures. Figures 10(a), (b), (c), and (d) show the temperature distribution for the straight-barrel structure, and conical barrel structures A, B, and C, respectively. It is observed that the maximum temperature is concentrated near the magnet rotor end of the conductor rotor, and with the increase in taper, the maximum temperature gradually decreases. Compared with the straight-barrel structure, the maximum temperatures in conical barrel structures A, B, and C are reduced by 7.77°C, 13.63°C, and 13.87°C, respectively. This demonstrates that the cooling effect of the conical barrel structure is superior, and improves as the taper increases. However, when the taper is too large, the thickness of the yoke iron near the magnet rotor end becomes thinner, resulting in poorer thermal conduction and a smaller reduction in temperature.

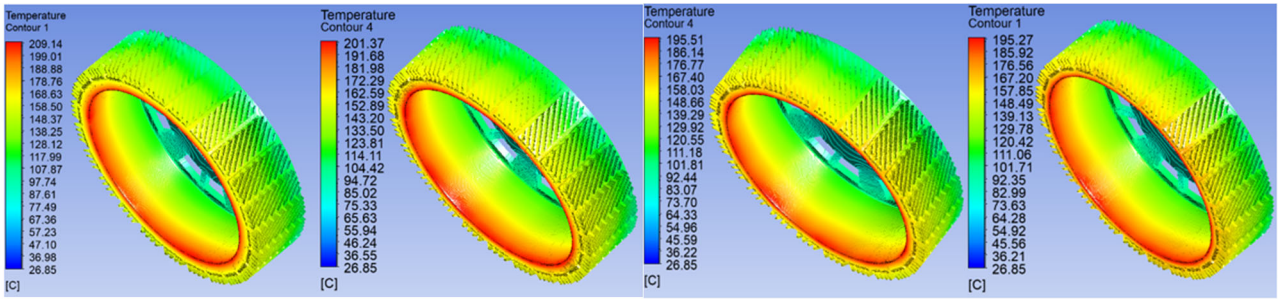

(a)Straight tube structure (b)A model (c)B model (d)C model

Figure 10. Conductor rotor temperature distribution under different structures

4.4. Surface Heat Transfer Coefficient

Figure 11 shows the distribution of the surface heat transfer coefficient under maximum thermal power loss for different conductor rotor structures. Figures 11(a), (b), (c), and (d) display the heat transfer coefficient distribution for the straight-barrel structure, and conical barrel structures A, B, and C, respectively. Since the surface heat transfer coefficient is related to the surface air flow speed and the temperature difference, the straight-barrel structure surface, with similar air flow speeds and greater temperature differences near the magnet rotor, forms layers. The maximum heat transfer coefficient can reach 75.20W/(m·°C), with an average surface heat transfer coefficient of 29.15W/(m·°C). For conical barrel structure A, due to the gradient formed by the air flow speed and the larger temperature difference near the magnet rotor, layers form, but the surface temperature is lower compared to the straight barrel, hence the maximum heat transfer coefficient only reaches 72.37W/(m·°C). The average surface heat transfer coefficient is 30.58W/(m·°C), overall providing better cooling than the straight-barrel structure. The maximum heat transfer coefficient for conical barrel structure B reaches 60.17W/(m·°C), with an average surface heat transfer coefficient of approximately 34.73W/(m·°C). For conical barrel structure C, due to the relatively small decrease in temperature compared to structure B and a significant increase in surface air flow speed, the maximum heat transfer coefficient reaches 75.31W/(m·°C), with an average surface heat transfer coefficient of approximately 38.61W/(m·°C), overall offering superior cooling compared to the straight-

barrel structure. Moreover, as the taper increases, the maximum heat transfer coefficient fluctuates, but the average heat transfer coefficient increases with the taper, enhancing the overall cooling effect.

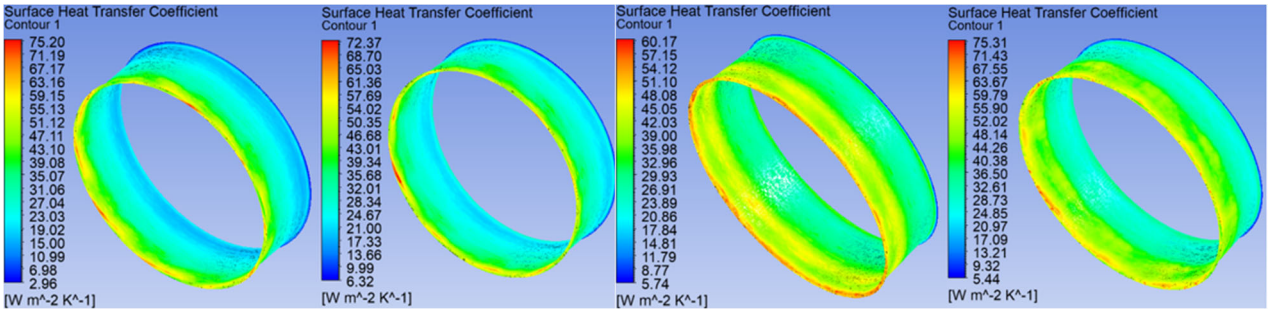

(a)Straight tube structure (b)A model (c)B model (d)C model

Figure 11. Distribution of the conductor surface velocity vector under different structure

5. Conclusion

Simulation results reveal that, without altering the outer diameter of the permanent magnet speed regulator and the volume of the permanent magnet, the conical permanent magnet speed regulator possesses the following advantages:

1)At low slip, the maximum output torque and speed of the conical structure with trapezoidal permanent magnets are slightly higher than those of the cylindrical speed regulator. It can provide higher power at low slip, meeting the speed regulator's requirements for rated power.

2)The overall trend of the speed regulation curve is similar to that of the cylindrical structure, having a minimal impact on the speed regulation effect. At maximum thermal power consumption, the coupling degree is higher, the air gap is larger, and the maximum unit volume heating power is lower.

3) In the process of adjusting to reduce the coupling degree, the increased air gap of the conical structure provides more cooling space, making it more suitable for speed regulation situations with quadratic loads.

4)At high thermal power consumption, due to the structural specificity, the conical structure forms a velocity gradient, increasing the surface air flow speed, and the flow speed changes with the temperature gradient direction, improving the cooling conditions. The higher the taper of the conical speed regulator, the lower the temperature of the conductor rotor, allowing the conductor rotor to operate safely at lower temperatures.

References

[1] Wang J, Wang D, Wang S, et al. A Review of Recent Developments in Permanent Magnet Eddy Current Couplers Technology[C]//Actuators. MDPI, 2023, 12(7): 277.

[2] Zhu Y, Wang H, Li H, et al. Transmission Performance of Halbach Array Cylindrical Permanent Magnet Governor[J]. Electronics, 2023, 12(5): 1161.

[3] Guo L Z, Yao T, Li X Y, et al.Research on heat dissipation of cylindrical permanent magnet speed regulator based on magnetothermal coupling simulation [J]. Mechanical Manufacturing and Automation, 2020,49(02):146-149.

[4] Wang B. Heat dissipation design and analysis of air-cooled permanent magnet eddy current speed regulator[D]. Nanjing University of Science and Technology, 2018.

[5] Li Y, Lin H, Yang H, et al. Analytical analysis of a novel flux adjustable permanent magnet eddy-current coupling with a movable stator ring[J]. IEEE Transactions on Magnetics, 2017, 54(3): 1-4.

[6] Wu P X. Heat dissipation design and analysis of air-cooled permanent magnet eddy current speed regulator[D]. Nanjing University of Science and Technology, 2018.

[7] Li, G. K., Jia, R. Z. & Ji, Q. S. Magnetic drive and magnetic pump[J]. Journal of the Chinese Society of Rare Earths, vol. S1 534–537 (1994).

[8] Teng W, Zhenghui W, Yipeng W, et al. Speed Regulation Characteristics of Variable Conductivity-Based Barrel-Type Permanent Magnet Eddy Current Governor[J]. IEEE Access, 2023, 11: 30159-30170.

[9] Sun Z S, Li X Q, Li X N. Research and application of permanent magnet eddy current speed regulator[J]. Mechanical Manufacturing and Automation, 2016, 45(3): 1-4.

[10] Sun Z S, Zhou L P, Wang X D, et al. Research on magnetic field analysis and characteristics of cylindrical permanent magnet speed regulator [J]. China Mechanical Engineering, 2015, 26(13): 1742-1747.

[11] Gulec M, Aydin M, Nerg J, et al. Magneto-thermal analysis of an axial-flux permanent-magnet-assisted eddy-current brake at high-temperature working conditions[J]. IEEE Transactions on Industrial Electronics, 2020, 68(6): 5112-5121.

[12] Zhu Y, Wang L, Liu H. Study on temperature field of high-power permanent magnetic coupling rotating centrifugal water cooling [J]. Machine Tool & Hydraulics, 2021, 49(13) : 171－174.

[13] Wang L, Jia Z, Zhu Y, et al. Flow field and temperature field of water-cooling-type magnetic coupling[J]. Chinese Journal of Mechanical Engineering, 2019, 32: 1-12.

[14] Wang S, Ma X, Hu Z, et al. Multi-Parameter Optimization of Heat Dissipation Structure of Double Disk Magnetic Coupler Based on Orthogonal Experimental Design[J]. Energies, 2022, 15(23): 8801.

[15] Pupin V, Orlov V. Mathematical Calculation of Synchronous Electric Motors Dynamic Stability[J]. Mathematics, 2023, 11 (21): 4465.